Leveraging Synthetic Aperture Radar (SAR) to improve above-normal flow prediction in ungauged basins

Shiqi Fang[1], J. Michael Johnson [2], and A. Sankarasubramanian[1]

[1] Department of Civil, Construction and Environmental Engineering, North Carolina State University, Raleigh, NC, USA
[2]Lynker, Fort Collins, CO, USA

Corresponding author: Shiqi Fang (sfang6@ncsu.edu)

Key Points:

- We integrate SAR data with the NWM to enhance predictions of above-normal flow in ungauged basins, improving accuracy and reliability
- The model results in significant improvements in predictive accuracy, particularly in areas lacking comprehensive streamflow measurements
- STHM-SAR model integrates predictors and GFDS-SAR data, enhancing 86% of natural basin sites and 76% of coastal basin sites' predictions.

Abstract

Effective flood prediction significantly enhances risk management and response strategies, yet remains challenging, particularly in ungauged basins. This study investigates the capacity for integrating streamflow derived from Synthetic Aperture Radar (SAR) and U.S. National Water Model (NWM) output to provide enhanced predictions of above-normal flow (ANF). Leveraging the Global Flood Detection System (GFDS) and Principal Component Regression (PCR) of SAR data, we apply the Spatial-temporal Hierarchical model (STHM) for ANF prediction replacing antecedent streamflow with SAR-derived flow. Our evaluation shows promising results, with STHM-SAR significantly improving prediction accuracy of NWM, especially coastal regions where approximately 60% of sites demonstrated enhanced performance compared to previous efforts. Spatial and temporal validations underscore the model's robustness, with SAR data contributing to explained variance by 24% on average. This approach not only streamlines post-processing modeling but also uniquely combines existing data, showcasing its potential to improve hydrological modeling, particularly in regions with limited measurements.

Plain Language Summary

This study explores improving flood prediction accuracy, which is vital for effective risk management and response planning. It focuses on integrating Synthetic Aperture Radar (SAR) data and the U.S. National Water Model (NWM) to predict above-normal flow (ANF). By combining SAR and NWM data using advanced techniques like the Global Flood Detection System (GFDS) and Principal Component Regression (PCR), a Spatial-temporal Hierarchical model (STHM) was developed. This model showed promising results, especially in coastal regions, with SAR data contributing significantly to the model's accuracy. This approach streamlines the modeling process and showcases the potential of combining existing data sources to improve hydrological modeling, particularly in regions with limited measurements.

1. Introduction

Developing accurate flood prediction models provides critical information to ensure sustainable flood risk management, early warning systems, and lifesaving responses (Johnson et al., 2016; Maidment, 2009). In the United States, the NOAA Office of Water Prediction provides runoff forecasts for the entire river network of the United States (National Weather Service, 2022; Salas et al., 2023) through the National Water Model (NWM). The NWM forecasts are used to generate flood inundation maps (Johnson et al., 2019) which are being used by River Forecasting Centers to provide operational guidance during flood events. However, the operational skill can still benefit from improved above-normal flows (defined as exceeding the 67^{th} percentile flow, ANF) as the raw NWM outputs suffer from both marginal and conditional biases (Johnson et al., 2023).

Postprocessing model outputs has been shown to enhance the forecast skill, however, NSEs of forecasts for ANF conditions near gauged locations are only skilled in 50% of evaluated basins (Fang et al., 2024; Frame et al., 2021; Johnson et al., 2023). The ability to predict above-normal flows is likely worse in ungauged basins highlighting the need for improved ANF prediction and the opportunity for utilizing using the unprecedented availability of NWM forecasts as a starting point.

Recent advancements in remote sensing (RS) data have emerged as a viable alternative to supplement *in situ* observations and process-based models (Sogno et al., 2022). Studies show they can benefit real-time forecasting capabilities, particularly in estimating the current stage and discharge (Van Dijk et al., 2015). RS data have been an important component of the Global Flood Monitor System (GFMS), which has been running in real-time for the last few years with results (including rainfall, flood, and Tropical Cyclone) being displayed at the NASA TRMM website (http://trmm.gsfc.nasa.gov/). The GFMS uses satellite-based estimates of precipitation to estimate runoff generation, routing, and flood inundation attributes such as stage. However, the challenge is effectively translating RS data into accurate streamflow forecasts in ungauged basins, despite its role in systems like the Global Flood Monitor System (GFMS) with the potential for real-time streamflow forecasting.

Streamflow forecasts can also be developed using process-based models (Archfield et al., 2015; Clark et al., 2015; Wood et al., 2011) and/or data-driven models (Kratzert et al., 2019). Traditionally Process based models have been used to tackle the "grand challenge of hydrology" of achieving consistence hydrologic prediction everywhere on earth (Sperna Weiland et al., 2012; Wood et al., 2011). And while efforts have substantially improved these modeling paradigms, successfully achieving accurate hydrologic prediction everywhere remains a challenge due to difficulties in estimating and maintaining antecedent conditions. Process-based models can utilize remotely derived variables like precipitation, soil moisture, and evapotranspiration (AghaKouchak et al., 2015; Vinukollu et al., 2011). To this end, there are numerous studies focused on incorporating synthetic, in situ, or remote sensing-derived water level observations into forecasting systems (Mazrooei et al., 2019; Mazrooei et al., 2021). For example, Revilla-Romero et al. (2016) utilized the ensemble Kalman filter to integrate low-resolution satellite-based flood extents from the GFDS into a global forecasting system aimed at real-time flood forecasting.

While streamflow can be derived from remote sensing instruments, e.g., MODIS (Sahoo et al., 2022; Tarpanelli et al., 2019) or LANDSAT (Gleason et al., 2014) these sensors provide lower spatial resolution and can be impeded by clouds and other obstacles - particularly in periods of above-normal or high flows (Alquraish and Khadr, 2021). On the other hand, technologies such as synthetic aperture radar (SAR) can provide high-resolution images of water conditions, even in adverse weather conditions ((Tsokas et al., 2022; Yoon et al., 2022). Streamflow estimation using SAR data usually involves building empirical relationships between ground-measured streamflow and the SAR data to estimate above-normal/high flow signal(Yoon et al., 2022); a curve number approach by estimating runoff from rainfall amounts (Beck et al., 2009; Hong and Adler, 2008); or a histogram thresholding or clustering method to separate flooded from non-flooded areas in SAR imagery (Martinis et al., 2009). Hostache et al. (2018) employed a modified Particle Filter with Sequential Importance Sampling to integrate probabilistic flood maps from SAR into a hydrologic and hydraulic model, while Cooper et al. (2018) demonstrated that assimilating SAR backscatter could outperform transforming it into water levels in their study. While the mentioned studies have demonstrated notable skill in predicting streamflow at a basin scale, their applicability on a continental scale (e.g., Coterminous US) has not been demonstrated to date. Largely, assimilating RS data into a process-based hydrological models at large scales is typically limited by computational time. In these cases, data-driven methods like Spatiotemporal Hierarchical Model (STHM) or Long short-term memory (LSTM) (Feng et al., 2020; Frame et al., 2021), can provide a hybrid approach that leverage remote sensing products and physics-based model outputs to inform statistical and machine learning models to combine the products into a n improved output. In 2023, Fang et al. introduced a STHM model that improved NWM streamflow predictions using a set of geospatial catchment characteristics and a three-day averaged streamflow observation (aggregated to the HUC8 watershed level). This study presented a hierarchical spatial-temporal model (STHM) that improves above-normal flow (ANF) prediction across CONUS basins, with significant enhancements in ANF prediction for most sites, while also facing challenges in predicting ANF for coastal basins and obtaining antecedent streamflow conditions for ungauged basins.

The aim of this study is to understand if the process based NWM, a suite of geospatial catchment characteristics, and SAR streamflow data can be integrated to improve on previous STHM efforts to provide improved ANF estimates. The paper is structured as follows: Section 2 outlines the materials and data used, Section 3 presents the results with a thorough analysis of the model's predictions, and Section 4 discusses the results, emphasizing research gaps and suggesting potential solutions to overcome challenges.

2. Materials and Methods

2.1 Hydroclimate and land use data

The NWM makes predictions across a modified version of the National Hydrographic Dataset (NHDPlusV2, McKay, 2012; Blodgett, 2023). To compare forecasts to observations, co-located common feature IDs and USGS National Water Information System (NWIS) gauges were extracted from the Routelink file associated with NWM v2.1. The dataRetrieval R package (De Cirro et al., 2018) was used to identify and retrieve streamflow data for sites with a minimum of 10 years of data between 1993 and 2018. Hourly simulations for NWM 2.1 were obtained using the "nwmTools" package (Johnson et al, 2023b, Johnson et al, 2021) and aggregated to a daily mean. Catchment characteristics were accessed from Johnson, et al., (2023), which summarized dam, hydroclimatic, land use, and anthropogenic characteristics to gage locations in the Gages II Network (Falcone, 2011). Furthermore, the GAGESII dataset includes the 2009 hydro-climatic network (HDCN) categories, distinguishing between controlled and natural basins. Lastly, the REACHCODE associated with the NHDPlusV2 COMID enables the identification of Hydrologic Unit Code (HUC) regions provided by the Watershed Boundary Dataset. All the above-mentioned data can be accessed at https://github.com/LynkerIntel/nwm-evaluation-2023.

2.2 Water Surface Metrics from GFDS–SAR

The Global Flood Detection System (GFDS) provides a flood monitoring system created by the Joint Research Centre of the European Commission in partnership with the Dartmouth Flood Observatory at Colorado University (https://www.gdacs.org/flooddetection/Download/Technical_Note_GFDS_Data_Products_v1.pdf).

The system integrates satellite measurements from sensors including the Tropical Rainfall Measuring Mission (TRMM), Global Precipitation Measuring (GPM), Advanced Microwave Scanning Radiometer-Earth (AMSRE), and AMSR2. These measurements are amalgamated to generate a variety of products displaying flood signals. GFDS water surface metrics have been instrumental in numerous studies (Van Dijk et al., 2016; Yoon et al., 2022). Moreover, various real-time flood monitoring applications rely on the data streams provided by GFDS.

GFDS estimates water surface metrics using brightness temperatures. If the physical temperature remains constant, changes in brightness can be assumed to be caused by changes in water in the pixel. Since the raw values are influenced by factors such as physical temperature, permittivity, surface roughness, vegetation, atmospheric moisture, and other environmental variables (Kugler and De Groeve, 2007; Van Dijk et al., 2016), $T_{b,measurement}$ is scaled by the signal of land observation of surface temperature.

An M/C value can be defined as the ratio of measurement/wet signal ($T_{b,measurement}$t) over calibration/dry observations, which is detected by SAR as water surface signal for proxy streamflow:

$$s = \frac{M}{C} = \frac{T_{b,measurement}}{T_{b,calibration}} \qquad (1)$$

where, T_b is passive microwave radiometers, brightness temperature, subscript "measurement" and "calibration" M and C, respectively. These can be accessed from GFDS website (https://www.gdacs.org/flooddetection/DATA/SINGLE/SignalTiffs/).

2.3 Principal Component Regression (PCR) of M/C ratio

Since the M/C ratio provided by GFSD is spatially explicit, we use Principal Component Analysis (PCA) to reduce the dimension to estimate the conditions of a given river. Principal Component Analysis (PCA) helps convert the correlated time series available at multiple grid points into orthogonal components, so that fewer components can explain the observed variance across space. For each gauged location, we retain two components of brightness temperature (T) by performing PCA on the 24 nearest GFDS grid cells and developed a regression with the observed depth of daily streamflow (discharge divided by the drainage area). When doing this. we pool stations by HUC08 (See Figure 1 for detailed steps). Thus, each HUC8 will have a unique regression that can convert the PCs of the M/C ratio available for any given location to estimate the depth of streamflow at ungauged locations. By utilizing Principal Component Analysis (PCA) to reduce the dimensionality of the M/C ratio from GFDS data, we can effectively capture the essential features for estimating streamflow conditions in ungauged basins.

Thus, PCR is that after choosing two PCs that is indexed as "*g*", the important features of *X* have been retained by score matrix (T_g) (Camps-Valls and Bruzzone, 2005), and then applied a multiple linear regression (MLR) with T_g instead of *X* (M/C ratio) for calibration data matrix Y (observed depth of daily streamflow):

$$y = T_g C + \epsilon (2)$$

Where, the coefficient of regression (C) is given by:

$$\hat{C} = \left(T_g^T T_g\right)^{-1} T_g^T y \quad (3)$$

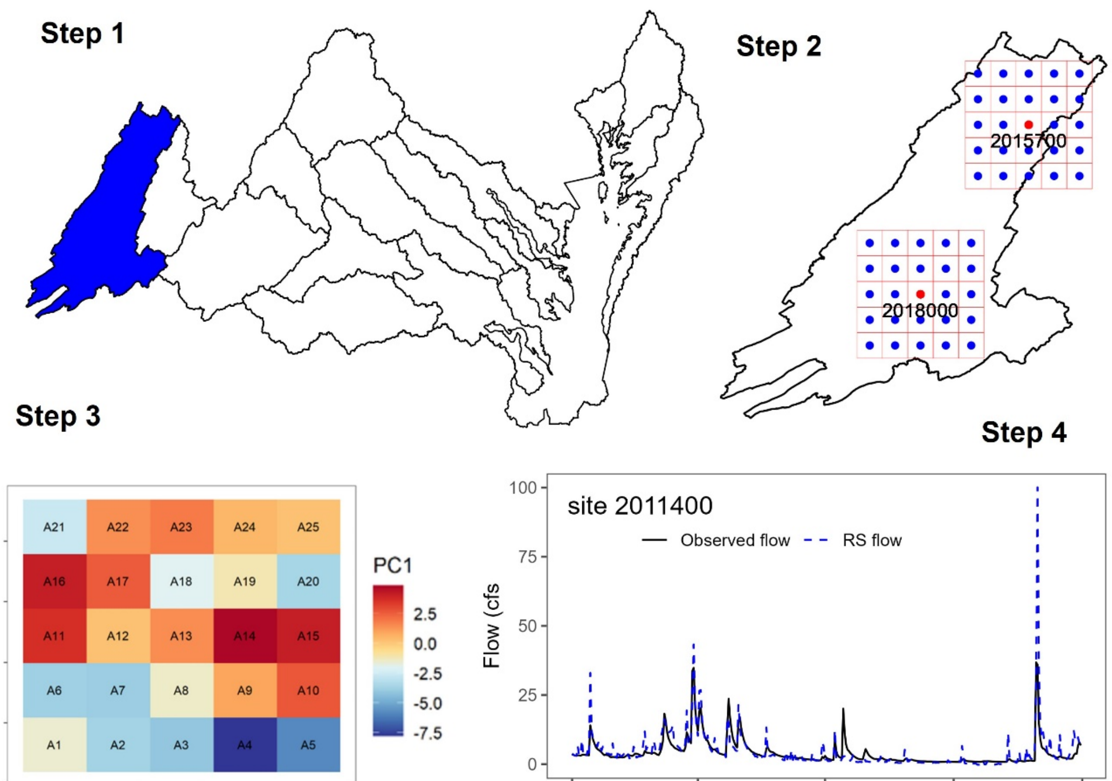

Figure 1. Key steps of deriving satellite remotely sensed ANF signals to streamflow. Step 1: Identify all Gages-II basins, grouped within the same HUC8 (colored in blue); Step 2:

Sampling M/C data for the gauged location and the 24 neighboring cells; Step 3: Principal Component regression for neighbors is applied; Step 4: Using top 2 a a polynomial regression is defined as described in Equation 2.

2.4 Spatial-temporal Hierarchical model for above-normal flow prediction using SAR data (STHM-SAR)

The aim of the study is to use SAR-estimated streamflow to further advance post processing techniques that can be applied to large scale process-based models. Here we start with the STHM defined in Fang et al, 2024 and replace the 3-day area-weighted gaged flows with the SAR-derived streamflow for the previous 3 days. Thus the new SAR informed STHM-SAR can be written as:

$$Q_{\{t(\tau,i,j,k)\}} = \beta_{\{000,\tau\}} + \beta_{\{1(\tau,i,j,k)\}} Q^{NWM}_{\{t(\tau,i,j,k)\}} + \beta_{\{2(\tau,i,j,k)\}} Q^{SAR}_{\{t(\tau,i,j,k)\}} + \beta_{\{01(\tau,j,k)\}} PET_{\{\tau(j,k)\}} + \beta_{\{001,\tau\}} AI_{\{i(j,k)\}} + \beta_{\{002,\tau\}} Imp_{\{i(j,k)\}} + \beta_{\{003,\tau\}} \rho_{\{i(j,k)\}} + \varepsilon_{\{t(\tau,i,j,k)\}} \quad (4)$$

where, Q^{NWM} is the NWM daily flow; ρ is the Spearman correlation indicating moisture and energy being in-phase or out-phase; PET is the mean 10-day potential evaporation as mentioned above; S is the upstream total dam storage; AI is the aridity index; *Imp* is the percent impervious; and ε is the residual.

2.5 Model evaluation

To evaluate the skill of our model, we use the Nash–Sutcliffe efficiency (NSE) metric which is widely used to measure the predictive skill of hydrological models (McCuen et al., 2006). In a perfect model with an estimation error variance equal to zero, the resulting NSE equals 1. A model with an estimation error variance equal to the variance of the observed time series, results in an NSE of 0. Conversely, an NSE less than zero occurs when the observed mean is a better predictor than the model. The model performance criteria recommended by Moriasi et al. (2007) was used for evaluating performance meaning predictions were considered “acceptable” if NSE scores are greater than 0.5 and “good” if the NSE is above 0.67.

Since we are interested in assessing the performance of the model for estimating flows in ungauged locations, we use both spatial and temporal validation procedures similar to that of Fang et al., (2024). For spatial validation, we used a k(20)-fold cross-validation method (Browne, 2000) treating 5% of locations as ungauged within each hierarchical group and fit the remaining 95% of stations for the period 1993 and 2018. We evaluated the STHM-SAR performance for the period 2009 to 2018 for the left-out basins. This process of leaving out 5% of the basins is repeated until all evaluated in a cross-validation mode. The temporal validation is performed to evaluate the STHM-SAR performance over a period different from the calibration, whereas the spatial validation is performed to evaluate the STHM-SAR for application in ungauged basins. The temporal validation is performed by calibrating the STHM-SAR model using the data from 1993 to 2008 with the remaining data from 2009 to 2018 being considered for validation. Thus, all the reported model evaluation, NSEs in Figures 2-4, are for the period 2009 to 2018 based on k(20-fold cross-validation.

3. Results

We first evaluated the correlation between GFDS SAR-derived and observed daily streamflow across all natural basins (Figure 2) and also calculated the NSE between the 3-day average streamflow from the GFDS-SAR and observed 3-day average streamflow (Y axis) (Figure 3). Figure 3a also compares the NSE from the GFDS-SAR with the NSE (X-axis) between the 3-day average streamflow estimated based on the simple depth of streamflow (i.e., without using the GFDS-SAR stage estimates) with the observed streamflow. We then conducted an analysis of model performance using SAR-derived data (Figure 4) and present an examination of contributing factors in the STHM-SAR compared to the base STHM (Fang et al., 2024).

3.1 SAR-derived streamflow represents observed streamflow moderately well

The correlation between SAR-derived and observed discharge varies across the CONUS is important to understand when looking to use SAR-derived products as a proxy for flow prediction (Figure 2), but Figure 2 shows improvement in estimating 3-day streamflow using the SAR-derived streamflow when compared with the 3-day streamflow estimated using the simple depth of streamflow. The correlation between SAR-derived streamflow and observed above average streamflow is notably strong, as depicted in Figure 2. Across all Gages-II basins, the mean correlation exceeded 0.53 for high flows during validation, underscoring the reliability of the SAR-derived streamflow. Spatially, the Northwest regions exhibited the highest correlation, while the lowest correlation was observed around the 95th meridian (Seager, 2017; Johnson et al 2023a; Johnson et al 2023b). Notably, the Tennessee River Basins demonstrated limited performance by using SAR-derived high streamflow. Prior work from Van Dijk et al. (2016) suggested that the most successful sites (with R > 0.8) are concentrated in the southeast of the USA. However, their focus was on the entire daily streamflow time series whereas we focus primarily in estimating high flows in Figure 2.

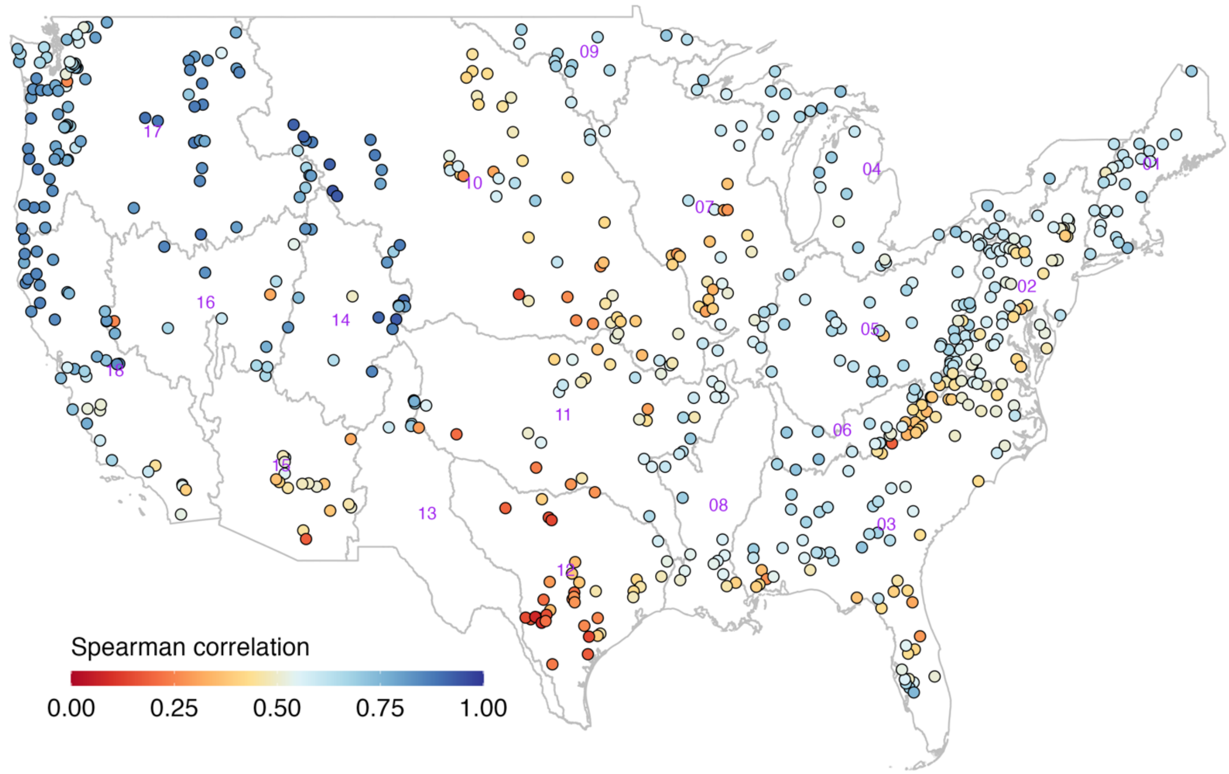

Figure 2. Spearman Rank correlation between above average SAR-derived and observed streamflow (all conditions) for Gages-II basins during the validation period (2010-2018).

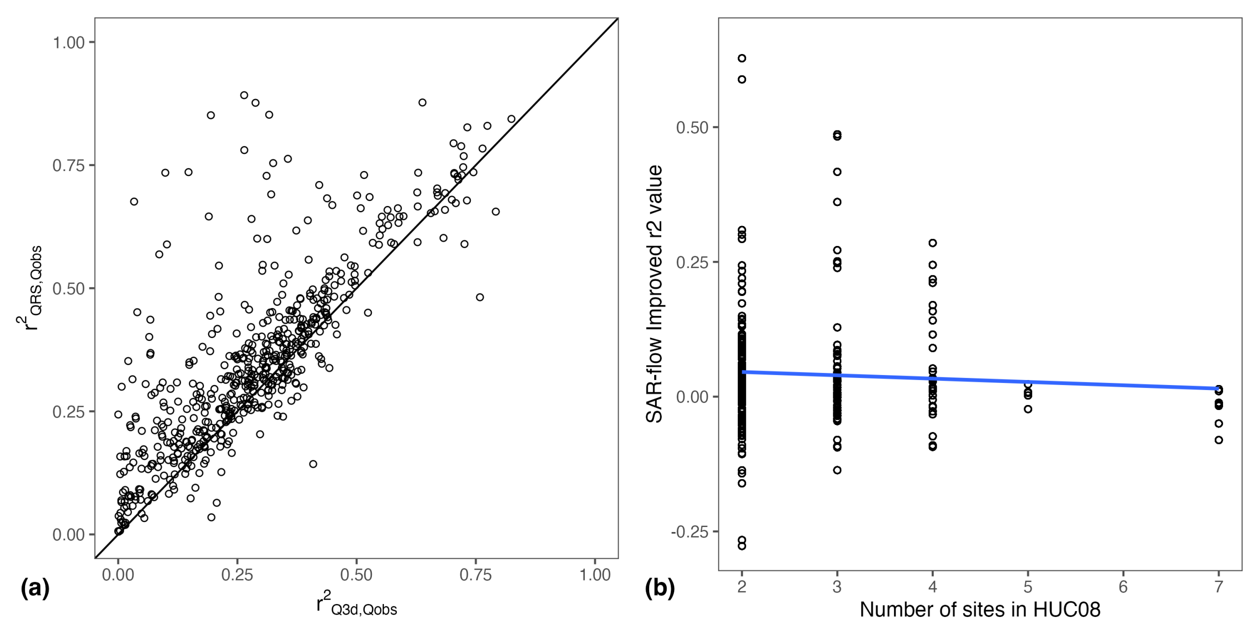

Figure 3 Left: SAR-derived streamflow compared with previous 3-day streamflow as the antecedent condition in Fang et al. 2024 by comparing the r-squared values with observed

streamflow. Right: SAR-derived streamflow r-squared values improvements from previous 3-day streamflow relationship as the number of sites within the same HUC08.

The analysis conducted in Fang et al. (2024), comparing the R-squared values between GFDS SAR-derived streamflow and the 3-day average streamflow estimated from the simple depth method, demonstrates that GFDS-SAR derived streamflow consistently surpasses the performance of the simple depth approach in explaining the variability observed in streamflow (see Figure 3a). This suggests that GFDS-SAR derived streamflow better captures the underlying variability in streamflow dynamics compared to the traditional 3-day flow approach. Moreover, Figure 3b shows that the improved performance of SAR derived streamflow decreased as the number of gauges increases in the same HUC08. The relationship underscores that these performance enhancements are notably more significant in basins with limited gauged locations, where 29% of these basins with ≤ 2 gauges often located within coastal basins (<150km along coastal line, Fang et al. 2024).

3.2 STHM-SAR improves above-normal streamflow predictions

Next we look more closely at how the STHM-SAR enhances NWM predictions in ANF events (as illustrated in Figure 4). The results show 81.6% of the sites exhibit improved skill compared to the NWM alone. Most of these improved sites were concentrated in HUC2 regions (01-06, 15-18 as shown in Figure 2). The most substantial enhancements were observed in the northwest regions, where over 85% of the sites exhibited NSE values greater then 0.67. In comparison with the findings of the gage aggregated STHM, the STHM-SAR demonstrated notable improvements, particularly in coastal sites, showcasing an average NSE improvement of 0.15. This highlights the benefits of refining predictions with RS inputs to better predict high-flow events. The accuracy of streamflow forecasting provides the capability for continuous adjustments and updates to the forecast as new and relevant data becomes available (for example through the Next Generation Water Resource Modeling Framework (Odgen, 2021, https://www.weather.gov/media/owp/oh/docs/2021-OWP-NWM-NextGen-Framework.pdf). This adaptability is crucial for maintaining the forecast's precision and relevance.

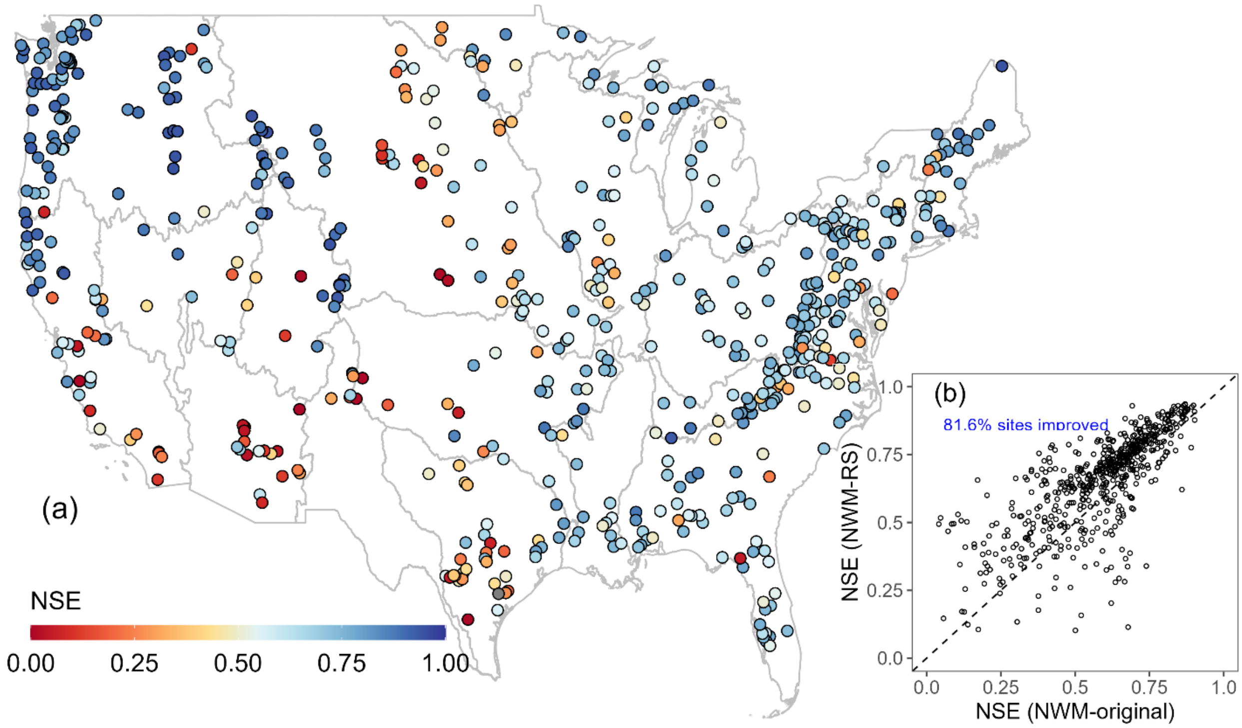

Figure 4 (a) Spatial distribution of NWM (RS) model predicted high streamflow (>67%) multiple years average performance (as in NSE) for HCDN basins during calibration period (2010-2018); (b) NWM(RS) model predicted high streamflow (>67%) improvement (as in NSE performance) for each site compared with NWM (original) streamflow during calibration period (2010-2018).

3.3 STHM-SAR predictors' contribution

The STHM-SAR model, incorporating all predictors from Fang et al., (2023) along with the 3-day average streamflow estimated from GFDS-SAR estimates, resulted in improvements in 86% of sites from natural basins, and 76% of sites from coastal basins. To better understand the impact of individual predictors, each predictor was assessed using the relative importance estimator proposed by Grömping (2007) (Figure 5). The NWM streamflow alone accounts for more ~43% of the variance in observed above-normal streamflow across the CONUS proving the value of having an operational, process-based model to draw on. Critically, this suggests that the NWM prediction is doing well at capturing variation in flow regimes but not magnitudes. SAR-derived flow contributes significantly as well, explaining 27% of the corresponding variance. The remaining predictors contribute between 5-12% of the observed streamflow variance, as depicted in Figure 5.

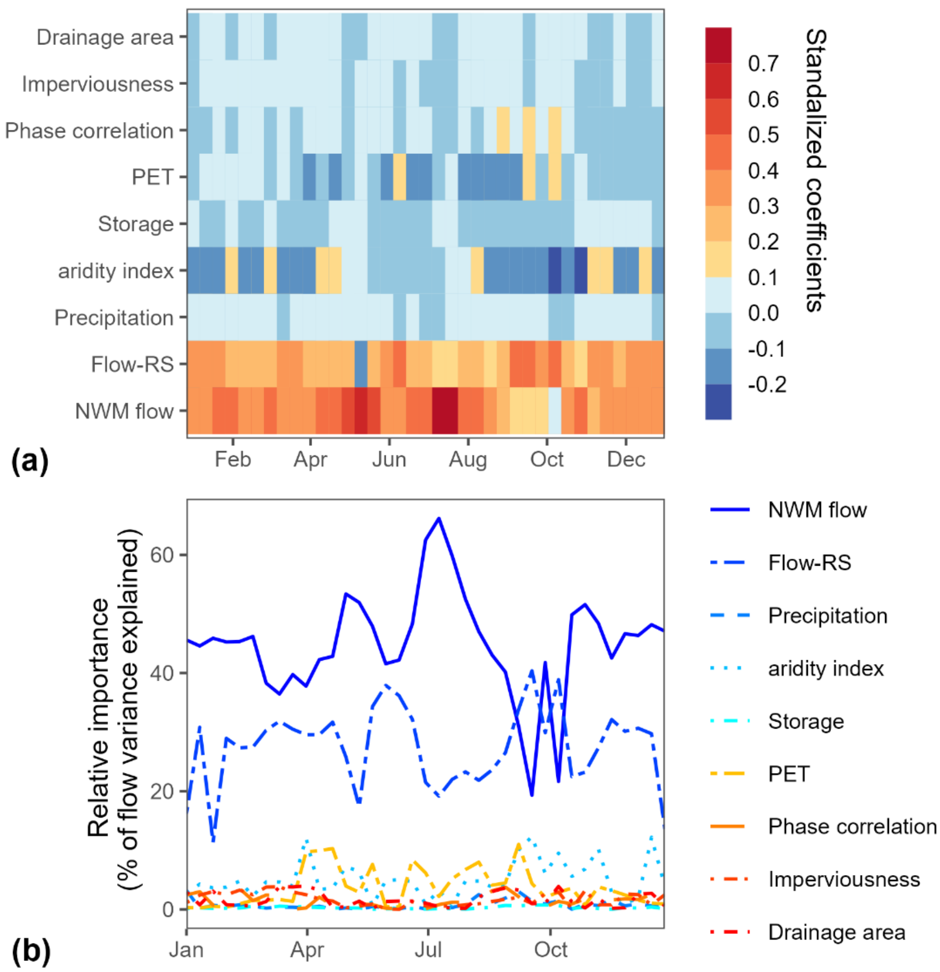

Figure 5. (a) Standardized model coefficients of selected predictor variables; (b) Overall average relative importance of selected predictor variables, expressed as % variance explained by the hierarchical model for HCDN basins.

From Figure 5a, it is evident that, apart from the coefficients associated with SAR-flow and NWM, the coefficients of other predictors were predominantly negative. This indicates an inverse relationship between these predictors and the observed streamflow. According to Figure 5b, the impact of individual hydroclimatic predictors on regionalization performance is relatively limited. In contrast, combinations of these predictors play a more substantial role, especially during specific periods. Notably, the combination of PET and aridity index together explained over 10% of the streamflow variance. This underscores the importance of considering specific combinations of hydroclimatic information, as they can substantially enhance the understanding and prediction of streamflow patterns across CONUS.

In Figure 5b, it is evident that NWM reanalysis streamflow predominantly contributes in explaining the observed streamflow variance particularly accounting for 54% overall on average in warmer seasons. Notably, SAR-flow provides better antecedent conditions, particularly when NWM experiences below-average performance in the summer and fall months.

This demonstrates the synergy between these predictors, where SAR-flow fills in the gaps and enhances predictive accuracy, ensuring a more reliable estimation. Particularly, during the months of June and September, SAR-flow becomes especially influential, explaining over 35% of the streamflow variance.

4. Discussion

The proposed STHM-SAR framework used the same model structure as STHM (Fang et al. 2024), while showing more local accuracy through improvements in antecedent conditions by replacing the previous subbasin averaged 3-day streamflow with SAR-derived flow. The results of our study confirm the effectiveness of the proposed framework in GAGES-II basins. The spatial calibration of the modeled streamflow, illustrated in Figure 4, indicates that a well-tuned model can improve predictive accuracy. One of the notable strengths of the suggested approach lies in its simplicity; it does not require complex models or additional predictors to enhance streamflow predictions and relies on open data and products. It leverages the inherent dynamics present in remote sensing data to effectively improve antecedent conditions as illustrated in Figure 5. This approach not only simplifies the post processing modeling process but also demonstrates the potential of utilizing existing data creatively to address challenges in hydrological modeling, especially in regions lacking comprehensive streamflow measurements (Figure 3).

The modeled above-normal streamflow, as depicted in Figure 4, aligns closely with the magnitude of the observed streamflow, surpassing the performance of STHM flow from Fang et al. 2023. This alignment underscores the utility of the proposed SAR-derived flow in better representing all locations across a diverse domain. This achievement is attributed to the integration of the correlation between the M/C ratio and observed flow from neighboring locations, accomplished through the PCR method. By leveraging these correlations, the SAR-derived flow not only captures the high streamflow patterns more effectively but demonstrates its capability in bridging the gap in data-scarce regions.

Compared with STHM (Fang et al. 2024), the substantial improvement in the STHM-SAR performance stems from the addition of SAR-derived data. Satellite products provide valuable information about ANF conditions that can complement or substitute in-situ readings. The increasing availability of high-resolution Earth Observation data, offered freely by numerous space agencies, opens avenues for enhancing above-normal flow forecasting and reanalysis based on Earth Observation.

5. Conclusion

The study demonstrates the effectiveness of integrating Synthetic Aperture Radar (SAR) data with the National Water Model (NWM) to enhance predictions of above-normal flow (ANF) in ungauged basins. The Spatial-temporal Hierarchical model for ANF prediction using SAR data (STHM-SAR) shows a significant improvement of 54% on average compared to previous STHM results (Fang et al., 2024), particularly benefiting coastal regions. The evaluation results indicate promising performance, with SAR data contributing substantially to explaining variance by 27% on average.

The correlation analysis between SAR-derived and observed streamflow highlights the reliability of SAR-derived streamflow as a proxy for flow prediction, especially during high-flow events. The STHM-SAR model, incorporating SAR-derived streamflow, outperforms the NWM alone, with 81.6% of sites showing improved skill. The spatial distribution of model-predicted high streamflow demonstrates significant enhancements, particularly in basins lacking gauged locations.

The contribution analysis of predictors in the STHM-SAR model emphasizes the importance of NWM reanalysis streamflow and SAR-derived flow, which together explain a significant portion of observed streamflow variance. The study underscores the value of considering specific hydroclimatic factors and leveraging remote sensing data to enhance flood prediction capabilities, especially in data-scarce regions and ungauged basins. Overall, the findings of this study highlight the potential of remote sensing data integration and suggest avenues for further research and improvements in flood prediction modeling, contributing to more effective risk management and response strategies.

Acknowledgments

We are grateful for the support from NSF projects EAR-2208562, DMS-2152887, and CBET-2151651.

Open Research

Data Availability Statement

The GFDL data can be accessed at

https://www.gdacs.org/flooddetection/DATA/SINGLE/SignalTiffs/

The complete data workflow including data download on S. Fang (2023)

https://doi.org/10.5281/zenodo.7574439 from Zenodo repository.

References

AghaKouchak, A., Farahmand, A., Melton, F.S., Teixeira, J., Anderson, M.C., Wardlow, B.D. and Hain, C.R. 2015. Remote sensing of drought: Progress, challenges and opportunities. Reviews of Geophysics 53(2), 452-480.

Alquraish, M.M. and Khadr, M. 2021. Remote-Sensing-Based Streamflow Forecasting Using Artificial Neural Network and Support Vector Machine Models. Remote Sensing 13(20), 4147.

Archfield, S.A., Clark, M., Arheimer, B., Hay, L.E., McMillan, H., Kiang, J.E., Seibert, J., Hakala, K., Bock, A. and Wagener, T. 2015. Accelerating advances in continental domain hydrologic modeling. Water Resources Research 51(12), 10078-10091.

Beck, H.E., de Jeu, R.A.M., Schellekens, J., van Dijk, A. and Bruijnzeel, L.A. 2009. Improving Curve Number Based Storm Runoff Estimates Using Soil Moisture Proxies. Ieee Journal of Selected Topics in Applied Earth Observations and Remote Sensing 2(4), 250-259.

Browne, M.W. 2000. Cross-validation methods. Journal of mathematical psychology 44(1), 108-132.

Camps-Valls, G. and Bruzzone, L. 2005. Kernel-based methods for hyperspectral image classification. IEEE Trans. Geosci. Remote Sensing 43(6), 1351-1362.

Clark, M.P., Fan, Y., Lawrence, D.M., Adam, J.C., Bolster, D., Gochis, D.J., Hooper, R.P., Kumar, M., Leung, L.R. and Mackay, D.S. 2015. Improving the representation of hydrologic processes in Earth System Models. Water Resources Research 51(8), 5929-5956.

Cooper, E.S., Dance, S.L., Garcia-Pintado, J., Nichols, N.K. and Smith, P.J. 2018. Observation impact, domain length and parameter estimation in data assimilation for flood forecasting. Environmental Modelling & Software 104, 199-214.

Fang, S., Johnson, J.M., Yeghiazarian, L. and Sankarasubramanian, A. 2024. Improved National-Scale Above-Normal Flow Prediction for Gauged and Ungauged Basins Using a Spatio-Temporal Hierarchical Model. Water Resources Research 60(1), e2023WR034557.

Feng, D., Fang, K. and Shen, C. 2020. Enhancing Streamflow Forecast and Extracting Insights Using Long-Short Term Memory Networks With Data Integration at Continental Scales. Water Resources Research 56(9), e2019WR026793.

Frame, J.M., Kratzert, F., Raney, A., Rahman, M., Salas, F.R. and Nearing, G.S. 2021. Post‐Processing the National Water Model with Long Short‐Term Memory Networks for Streamflow Predictions and Model Diagnostics. JAWRA Journal of the American Water Resources Association.

Gleason, C.J., Smith, L.C. and Lee, J. 2014. Retrieval of river discharge solely from satellite imagery and at-many-stations hydraulic geometry: Sensitivity to river form and optimization parameters. Water Resources Research 50(12), 9604-9619.

Hong, Y. and Adler, R.F. 2008. Estimation of global SCS curve numbers using satellite remote sensing and geospatial data. International Journal of Remote Sensing 29(2), 471-477.

Hostache, R., Chini, M., Giustarini, L., Neal, J., Kavetski, D., Wood, M., Corato, G., Pelich, R.-M. and Matgen, P. 2018. Near-Real-Time Assimilation of SAR-Derived Flood Maps for Improving Flood Forecasts. Water Resources Research 54(8), 5516-5535.

Johnson, F., White, C.J., van Dijk, A., Ekstrom, M., Evans, J.P., Jakob, D., Kiem, A.S., Leonard, M., Rouillard, A. and Westra, S. 2016. Natural hazards in Australia: floods. Climatic Change 139, 21-35.

Johnson, J.M., Fang, S., Sankarasubramanian, A., Rad, A.M., Kindl da Cunha, L., Jennings, K.S., Clarke, K.C., Mazrooei, A. and Yeghiazarian, L. 2023. Comprehensive Analysis of the NOAA National Water Model: A Call for Heterogeneous Formulations and Diagnostic Model Selection. Journal of Geophysical Research: Atmospheres 128(24), e2023JD038534.

Johnson, J.M., Munasinghe, D., Eyelade, D. and Cohen, S. 2019. An integrated evaluation of the National Water Model (NWM)–Height Above Nearest Drainage (HAND) flood mapping methodology. Nat. Hazards Earth Syst. Sci. 19(11), 2405-2420.

Kratzert, F., Klotz, D., Shalev, G., Klambauer, G., Hochreiter, S. and Nearing, G. 2019. Towards learning universal, regional, and local hydrological behaviors via machine learning applied to large-sample datasets. Hydrol. Earth Syst. Sci. 23(12), 5089-5110.

Kugler, Z. and De Groeve, T. 2007. The global flood detection system. Office for Official Publications of the European Communities, Luxembourg 45.

Maidment, D.R. 2009 FEMA flood map accuracy, pp. 1-10.

Martinis, S., Twele, A. and Voigt, S. 2009. Towards operational near real-time flood detection using a split-based automatic thresholding procedure on high resolution TerraSAR-X data. Nat. Hazards Earth Syst. Sci. 9(2), 303-314.

Mazrooei, A., Sankarasubramanian, A. and Wood, A.W. 2019. Variational assimilation of streamflow observations in improving monthly streamflow forecasting. Hydrology and Earth System Sciences Discussions 2019, 1-22.

Mazrooei, A., Sankarasubramanian, A. and Wood, A.W. 2021. Potential in improving monthly streamflow forecasting through variational assimilation of observed streamflow. Journal of Hydrology 600, 126559.

McCuen, R.H., Knight, Z. and Cutter, A.G. 2006. Evaluation of the Nash–Sutcliffe efficiency index. J. Hydrol. Eng. 11(6), 597-602.

National Weather Service 2022. National Weather Service - Office of Water Prediction.

Revilla-Romero, B., Wanders, N., Burek, P., Salamon, P. and de Roo, A. 2016. Integrating remotely sensed surface water extent into continental scale hydrology. Journal of Hydrology 543, 659-670.

Sahoo, D.P., Sahoo, B., Tiwari, M.K. and Behera, G.K. 2022. Integrated remote sensing and machine learning tools for estimating ecological flow regimes in tropical river reaches. Journal of Environmental Management 322, 116121.

Salas, J., Saha, A. and Ravela, S. 2023. Learning inter-annual flood loss risk models from historical flood insurance claims. Journal of Environmental Management 347, 118862.

Sogno, P., Klein, I. and Kuenzer, C. 2022. Remote Sensing of Surface Water Dynamics in the Context of Global Change—A Review. Remote Sensing 14(10), 2475.

Sperna Weiland, F., Van Beek, L., Kwadijk, J. and Bierkens, M. 2012. Global patterns of change in discharge regimes for 2100. Hydrology and Earth System Sciences 16(4), 1047-1062.

Tarpanelli, A., Santi, E., Tourian, M.J., Filippucci, P., Amarnath, G. and Brocca, L. 2019. Daily River Discharge Estimates by Merging Satellite Optical Sensors and Radar Altimetry Through Artificial Neural Network. IEEE Trans. Geosci. Remote Sensing 57(1), 329-341.

Tsokas, A., Rysz, M., Pardalos, P.M. and Dipple, K. 2022. SAR data applications in earth observation: An overview. Expert Systems with Applications 205, 117342.

Van Dijk, A.I.J.M., Brakenridge, G.R., Kettner, A.J., Beck, H.E., De Groeve, T. and Schellekens, J. 2016. River gauging at global scale using optical and passive microwave remote sensing. Water Resources Research 52(8), 6404-6418.

Van Dijk, S., Molloy, P., Varinli, H., Morrison, J. and Muhlhausler, B. 2015. Epigenetics and human obesity. International journal of obesity 39(1), 85-97.

Vinukollu, R.K., Wood, E.F., Ferguson, C.R. and Fisher, J.B. 2011. Global estimates of evapotranspiration for climate studies using multi-sensor remote sensing data: Evaluation of three process-based approaches. Remote Sensing of Environment 115(3), 801-823.

Wood, E.F., Roundy, J.K., Troy, T.J., Van Beek, L., Bierkens, M.F., Blyth, E., de Roo, A., Döll, P., Ek, M. and Famiglietti, J. 2011. Hyperresolution global land surface modeling: Meeting a grand challenge for monitoring Earth's terrestrial water. Water Resources Research 47(5).

Yoon, H.N., Marshall, L., Sharma, A. and Kim, S. 2022. Bayesian Model Calibration Using Surrogate Streamflow in Ungauged Catchments. Water Resources Research 58(1), e2021WR031287.